THE JOURNAL OF PHYSICAL CHEMISTRY C

Article

pubs.acs.org/JPCC

Insight into the Thermal Quenching Mechanism for $Y_3Al_5O_{12}:Ce^{3+}$ through Thermoluminescence Excitation Spectroscopy

Jumpei Ueda,*[,†,‡,§,∥] Pieter Dorenbos,[§] Adrie J. J. Bos,[§] Andries Meijerink,[∥] and Setsuhisa Tanabe[†]

[†]Graduate School of Human and Environmental Studies and [‡]Graduate School of Global Environmental Studies, Kyoto University, Kyoto 606-8501, Japan

[§]Luminescence Materials Research Group, section FAME-RST, Faculty of Applied Sciences, Delft University of Technology, 2629 JB Delft, Netherlands

[∥]Debye Institute, Utrecht University, 3508 TA Utrecht, Netherlands

ABSTRACT: $Y_3Al_5O_{12}$(YAG):Ce^{3+} is the most widely applied phosphor in white LEDs (w-LEDs) because of strong blue absorption and efficient yellow luminescence combined with a high stability and thermal quenching temperature, required for the extreme operating conditions in high-power w-LEDs. The high luminescence quenching temperature (~600 K) has been well established, but surprisingly, the mechanism for temperature quenching has not been elucidated yet. In this report we investigate the possibility of thermal ionization as a cause of this quenching process by measuring thermoluminescence (TL) excitation spectra at various temperatures. In the TL excitation (TLE) spectrum at room temperature there is no Ce^{3+}:$5d_1$ band (the lowest excited 5d level). However, in the TLE spectrum at 573 K, which corresponds to the onset temperature of luminescence quenching, a TLE band due to the Ce^{3+}:$5d_1$ excitation was observed at around 450 nm. On the basis of our observations we conclude that the luminescence quenching of YAG:Ce^{3+} at high temperatures is caused by the thermal ionization and not by the thermally activated cross over to the 4f ground state. The conclusion is confirmed by analysis of the positions of the 5d states of Ce^{3+} relative to the conduction band in the energy band diagram of YAG:Ce^{3+}.

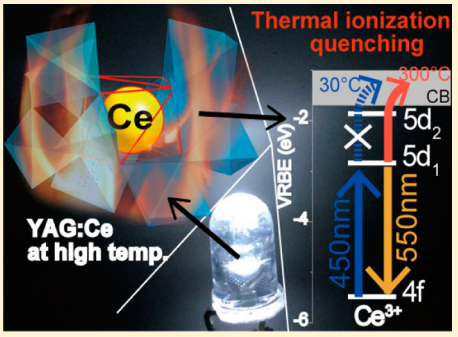

1. INTRODUCTION

White light LEDs (light-emitting diodes) are rapidly replacing incandescent lamps and (compact) fluorescent tubes in all lighting markets (consumer, automotive, and professional). This revolution in lighting has been enabled by the invention of the blue LED.[1] The most widely used type of white LEDs (w-LEDs) is a phosphor-converted w-LED (PC-LED), which is composed of an InGaN-based blue LED and visible light-emitting inorganic phosphors, such as oxides and nitrides doped with Ce^{3+} or Eu^{2+} as an active center.[2−4] The 5d−4f parity-allowed transitions of these active centers have several advantages in phosphors for w-LEDs, such as luminescence color variation and broad absorption and luminescence spectra with a large absorption cross section and high quantum efficiency.[5−10] These phosphors are required to have excellent thermal quenching behavior because the LED chip reaches temperatures up to ~200 °C in recent high-power w-LED applications.

Ce^{3+}-doped oxide garnets are the most prominent phosphor in w-LEDs. Since the discovery of YAG:Ce^{3+} as a LED-phosphor, many alternative phosphors have been designed;[11−14] but still, owing to the excellent spectral conversion characteristics, high stability under the extremely high photon flux and operating temperature, YAG:Ce^{3+} is applied in most w-LEDs and can be observed as a yellowish powder on top of the LED chip in w-LEDs. The thermal quenching temperature of the luminescence is a crucial parameter for LED phosphors. The excellent thermal quenching behavior of the Ce^{3+} luminescence in YAG:Ce^{3+} is well established, but the mechanism for thermal quenching remains unclear. In general, two processes of thermal quenching in Ce^{3+}-doped materials with the 5d−4f luminescence are considered.[15] One is the thermally activated cross over[16] from the 5d excited state to the 4f state; the other is the thermal ionization from the 5d excited state to the bottom of the conduction band (CB).[17] Thermally activated cross over is the nonradiative relaxation process from the 5d potential curve to the 4f ground potential curve through the crossing point in a configuration coordinate diagram. Thermal ionization is the thermally activated electron transfer process to the CB. Among various Ce^{3+}-doped garnets, $Gd_3Al_5O_{12}$ (GAG) and $Tb_3Al_5O_{12}$ (TAG) are suitable candidates of orange phosphors for warm white LEDs. However, the quenching temperature ($T_{50\%}$) of GAG:Ce^{3+} and TAG:Ce^{3+} is much lower than $Y_3Al_5O_{12}$(YAG):Ce^{3+}. Chiang et al. explained that the thermal quenching is caused by the difference of activation energies in the thermally activated cross-over process using a configuration coordinate diagram.[18] On the basis of the photoconductivity measurement as a

Received: September 10, 2015
Revised: October 8, 2015

DOI: 10.1021/acs.jpcc.5b08828
J. Phys. Chem. C XXXX, XXX, XXX−XXX

function of temperature and excitation wavelength, we demonstrated that the Ce^{3+}:5d−4f luminescence quenching in $Y_3Ga_5O_{12}$(YGG):Ce^{3+} and $Y_3Al_2Ga_3O_{12}$:Ce^{3+} is caused by autoionization and thermal ionization, respectively.[19] In our photoconductivity study up to 300 K it was found that the energy gap between the lowest 5d level ($5d_1$) of Ce^{3+} and the bottom of the CB decreases with increasing Ga content in $Y_3Al_{5-x}Ga_xO_{12}$:Ce^{3+}.[19] In other Ce^{3+}-doped Ga-substituted garnets such as $Gd_3Al_{5-x}Ga_xO_{12}$:Ce^{3+}[20] and $Ca_2LaZr_2Ga_3O_{12}$:Ce^{3+},[21] the luminescence quenching process was also determined to be thermal ionization due to the small band gap energy. However, the quenching process of YAG:Ce^{3+} with high band-gap energy has not yet been elucidated properly even though YAG:Ce^{3+} has been used as the main phosphor for general-purpose w-LEDs for almost 20 years.

The thermal quenching of the Ce^{3+} luminescence in YAG was already studied in 1973, when Weber measured the temperature dependence of the 5d−4f luminescence in YAG:Ce^{3+} and YAG:Pr^{3+} and reported that the lifetime of the $5d_1$ excited state rapidly decreases above 600 K in YAG:Ce^{3+}.[22] He tried to explain the quenching process by multiphonon emission from the 5d state to the 4f ground state. In 1991, Lyu and Hamilton reported a similar quenching curve ($T_{50\%} \approx 630$ K) based on lifetime measurements in YAG:Ce^{3+}.[23] Similar quenching curves have also been reproduced by Bachman and Meijerink et al., and they showed the $T_{50\%}$ increases above 700 K for very low Ce^{3+} concentrations.[24] From the rough agreement between the quenching activation energy (6500 cm^{-1}, 0.81 eV) and the $5d_1$-CB energy gap estimated from excited state absorption spectra (10 000 cm^{-1}, 1.24 eV),[23,25] Lyu and Hamilton suggested that the quenching process is caused by the thermal ionization. The energy location of the Ce^{3+} ground state with respect to the CB in YAG:Ce^{3+} was determined from photoconductivity measurements to be 3.8 eV[19,26] and from the vacuum-referred binding energy (VRBE) diagram presented by Dorenbos to be 3.78 eV.[27] By subtracting the 4f−$5d_1$ transition energy (457 nm, 2.71 eV) from these 4f-CB energy gaps, the $5d_1$-CB energy gap can be estimated to be approximately 1.1 eV, which is in line with the value of 1.24 eV estimated from the excited state absorption spectrum. The question is whether electrons in the $5d_1$ level can be transferred to the CB, i.e., over an energy barrier of approximately 1.1 eV by thermal stimulation at 600 K. In 2013, Ivanovskikh and Meijerink et al. constructed precise configuration coordinate diagrams for YAG:Ce^{3+}, YAG:Pr^{3+}, $Lu_3Al_5O_{12}$ (LuAG):Ce^{3+}, and LuAG:Pr^{3+} from low-temperature spectroscopy and compared the energy gap between the $5d_1$ level and the next lower 4f level with the 5d−4f luminescence quenching temperature in each sample.[28] On the basis of the good agreement between the configuration coordinate diagrams and the quenching temperature, they suggested that the quenching process of the 5d−4f luminescence in these materials is caused by the thermally activated cross-over process. However, there is no direct evidence of the thermally activated cross-over quenching process in YAG:Ce^{3+}.

In this study, we investigated the thermal quenching of YAG:Ce^{3+} by measuring thermoluminescence (TL) glow curves. TL is caused by detrapping of charges that were previously trapped followed by recombination on a luminescent center. Charge trapping occurs when electrons in the excited state of luminescence centers are transferred to the CB (e.g., through thermal ionization) and then captured by traps in the host. By measuring the TL intensity as a function of the charging wavelength, a TL excitation (TLE) spectrum is obtained that provides information on the threshold energy that causes the thermal ionization. Here, we measured the TL glow curves of YAG:Ce^{3+} as a function of charging wavelength and temperature and observed a $5d_1$ excitation band in the TLE spectrum above 573 K (300 °C), which is the onset temperature of the thermal quenching. This provides evidence that the onset of the thermal quenching of the Ce^{3+} luminescence coincides with thermally induced ionization. We will discuss the quenching process of YAG:Ce^{3+} in relation to the energy location of the Ce^{3+}:$5d_1$, $5d_2$ bands relative to the CB.

2. EXPERIMENTAL SECTION

For the synthesis of polycrystalline ceramics of $Y_3Al_5O_{12}$:Ce^{3+} (0.5% at the Y site), the chemicals Y_2O_3 (99.99%), Al_2O_3 (99.99%), and CeO_2 (99.99%) were used as starting materials. The powders were mixed by ball milling (Fritsch, Premium Line P-7) with ethanol. The obtained slurry was dried and pulverized and then pressed at 50 MPa into 10 mm-ϕ × 2 mm thick pellets. The pellets were sintered at 1600 °C for 6 h in vacuum. The crystal phase was identified as a single phase of the garnet structure using the X-ray diffraction measurement system (Rigaku, Ultima IV). Thermoluminescence (TL) measurements were performed with a RISØ TL/OSL reader model DA-15 and a controller model DA-20. The TL luminescence was detected with three 2 mm BG-39 filters (transmission between 320 and 650 nm) placed in front of an EMI9635QA photomultiplier tube (PMT). Samples were illuminated with monochromatic light obtained from a Xe lamp (Newport, 66921) and a monochromator (Newport, 74004). All measurements were performed under a flow of nitrogen gas. For the thermoluminescence excitation spectra (TLE), the samples were illuminated with the monochromatic light and after the illumination phase the TL glow curve was measured. The temperature dependence of photoluminescence (PL) was measured with the same RISØ TL/OSL reader model DA-15 and a QE65000 spectrometer from room temperature until 550 °C under 450 nm excitation. The temperature dependence of the lifetime was measured with Quantaurus-Tau (Hamamatsu Photonics, C11367-01) from 100 to 800 K under 340 nm picosecond LED excitation.

3. RESULTS AND DISCUSSION

To investigate the thermal quenching of Ce^{3+} luminescence, both the luminescence lifetime and the integrated intensity of Ce^{3+} luminescence were measured for YAG:Ce^{3+}(0.5%). Figure 1 shows the temperature dependence of (a) the Ce^{3+}:$5d_1$ lifetime and (b) the integrated $5d_1$-4f PL intensity for the luminescence band around 540 nm. From the lifetime data, the onset temperature of quenching ($T_{95\%}$) and the quenching temperature ($T_{50\%}$), which are the temperatures at which the lifetime (or PL intensity) become 95% and 50% of that at low temperatures, are estimated to be 580 (307 °C) and 668 K (395 °C), respectively. From the PL intensity, $T_{95\%}$ and $T_{50\%}$ are estimated to be 533 (260 °C) and 643 K (370 °C), respectively. $T_{50\%}$ from lifetime and PL intensity has a similar value and is in good agreement with the previous values of 650 and 630 K in YAG:Ce^{3+} reported by Weber and Lyu et al., respectively.[22,23] Compared with the $T_{50\%}$ (>700 K) in YAG:Ce^{3+} (~0.03%) reported by Bachman et al. the $T_{50\%}$ in our YAG:Ce^{3+} (0.5%) is lower, probably due to thermally

DOI: 10.1021/acs.jpcc.5b08828
J. Phys. Chem. C XXXX, XXX, XXX−XXX

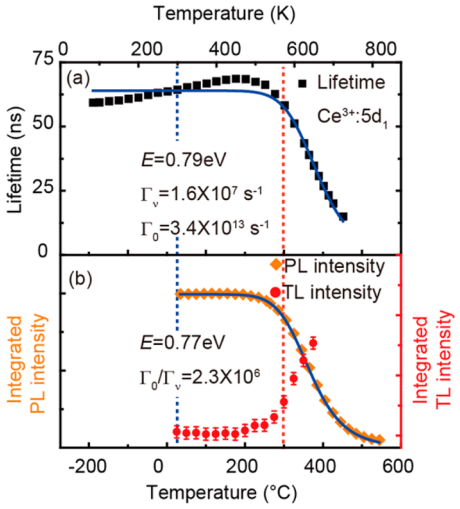

Figure 1. Temperature dependence of (a) Ce^{3+} luminescence lifetime (λ_{em} = 540 nm, for 340 nm excitation with a ps LED) and (b) integrated PL intensity and TL intensity for YAG:Ce^{3+}(0.5%). TL intensity was integrated between 623 (350 °C) and 773 K(500 °C) in each TL glow curve after 450 nm excitation at different temperatures from 303 (30 °C) to 648 K (375 °C). Blue and red dashed lines express the temperatures RT (no quenching) and 300 °C (onset of quenching), where the TLE experiments were conducted.

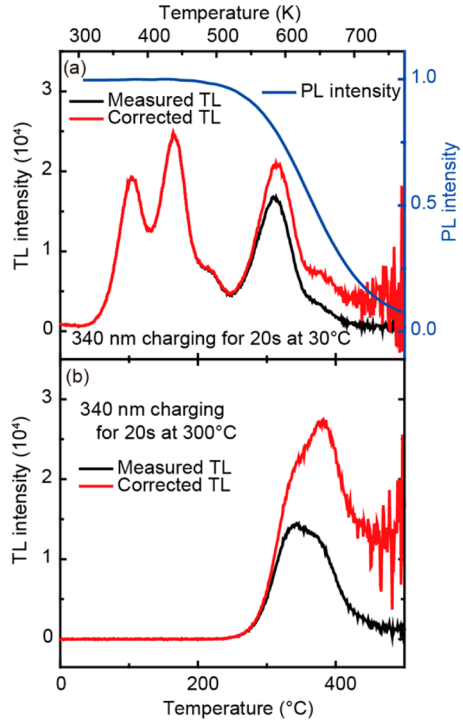

Figure 2. TL glow curves for YAG:Ce^{3+}(0.5%), as measured and corrected, after charging by 340 nm for 20 s at (a) 303 (30 °C) and (b) 573 K (300 °C). TL glow curves are recorded for 540 nm luminescence from Ce^{3+}. Black lines represent the glow curves as recorded. Red lines are glow curves after correction for the thermal quenching of the Ce^{3+} luminescence at high temperatures (blue line in a).

activated energy migration at higher concentration.[24,28] Activation energies are derived from the temperature dependence of lifetime and PL intensity according to the single-barrier quenching model, eqs 1 and 2, respectively

$$\tau(T) = \frac{1}{\Gamma_\nu + \Gamma_0 \exp(-E/kT)} \quad (1)$$

$$\frac{I(T)}{I_0} \approx \eta(T) = \frac{1}{1 + (\Gamma_0/\Gamma_\nu)\exp(-E/kT)} \quad (2)$$

where τ is the lifetime, I is the PL intensity, Γ_ν is the radiative rate, Γ_0 is the attempt rate of the nonradiative process, E is the activation energy, k is the Boltzmann constant, and T is the temperature. The activation energies from lifetime and PL intensity are found to be 0.79 ± 0.01 and 0.77 ± 0.01 eV, respectively, in good agreement with previous results.[23]

Thermoluminescence excitation (TLE) spectroscopy is a powerful tool to investigate if thermal ionization from the excited 5d state occurs.[29,30] The observation of a peak in a TL glow curve is direct evidence for thermal ionization. To establish if thermal ionization occurs upon photoexcitation at high temperatures, it is crucial that there are high-temperature TL peaks corresponding to deep traps that are stable at the high temperatures where thermal quenching is studied. In order to establish the presence of shallow and deep traps in the presently investigated YAG:Ce^{3+} samples, TL glow curves were recorded after excitation in the higher 5d band of Ce^{3+} at 340 nm. Figure 2 a and 2b shows the thermoluminescence (TL) glow curves after charging with 340 nm for 20 s in the YAG:Ce^{3+} sample at 303 (30 °C) and 573 K (300 °C). After charging at 573 K (300 °C), the sample was cooled down to room temperature and then TL glow curves were measured. The shape and maximum position of TL glow curves are modified by the thermal quenching of recombination luminescence.[27] Therefore, all TL glow curves were corrected by dividing the TL intensity by the Ce^{3+} PL intensity (blue line in Figure 2 a). The corrected TL glow curves are shown in red in Figure 2 a and 2b. In the corrected TL curve after charging at 303 K (30 °C), five TL peaks were observed with maxima T_m at 378 ± 1 (105 °C), 438 ± 1 (165 °C), 489 ± 1 (216 °C), 590 ± 1 (317 °C), and 657 ± 1 K (384 °C), which are referred to as traps 1, 2, 3, 4, and 5, respectively. From eq 3, based on first-order kinetics[31−33] and assuming a frequency factor, s, of 1 × 10^{11} s^{-1}[30] and a heating rate, β, of 5 K/s, trap depths E of the traps 1, 2, 3, 4, and 5 were roughly estimated to be 0.86, 1.00, 1.12, 1.36, and 1.52 eV, respectively

$$\frac{\beta E}{kT_m^{\,2}} = s \exp\left(-\frac{E}{kT_m}\right) \quad (3)$$

Similar TL peaks in YAG:Ce^{3+} were previously reported by other groups.[34−37] These TL peaks can be related to intrinsic defects in YAG:Ce^{3+}.

From the temperature quenching curves (Figure 1) it is clear that the luminescence in YAG:Ce^{3+} (0.5%) starts to quench at 573 K (300 °C), while at 303 K (30 °C) there is no quenching. To study the thermal ionization process, TL excitation (TLE) spectra were measured at both temperatures for excitation in the lowest d state ($5d_1$) at 450 nm and the next higher 5d state ($5d_2$) at 340 nm. In Figure 2, the TL glow peaks (traps 1−3) are absent after charging at 573 K (300 °C) because the traps involved are not stable at this high temperature. The traps responsible for the TL glow peak at 590 K (trap 4) have an electron trap depth distribution, and only the deepest ones are sufficiently stable to appear in Figure 2b. In order to compare the TLE spectra at 573 (300 °C) and 308 K (30 °C), only the TL intensity related to trap 5, integrated between 623 (350 °C)

DOI: 10.1021/acs.jpcc.5b08828
J. Phys. Chem. C XXXX, XXX, XXX−XXX

and 773 K (500 °C), is taken into account. The TLE spectra obtained are shown in Figure 3. At 303 K (30 °C) a TLE band

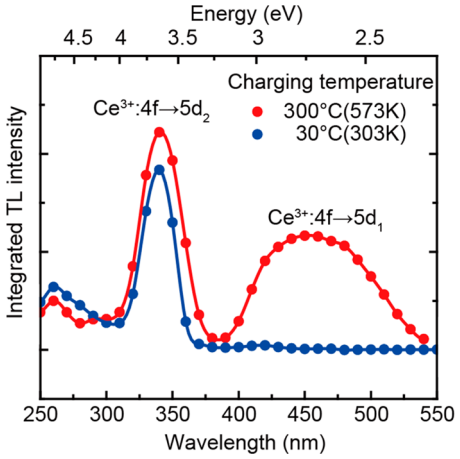

Figure 3. Thermoluminescence excitation (TLE) spectra at two charging temperatures: 303 (30 °C) and 573 K (300 °C). TLE spectra were recorded by measuring the integrated intensity for the high-temperature TL peak around 657 K for different excitation wavelengths between 250 and 550 nm with 20 s charging time.

is observed at around 340 nm, while at 573 K (300 °C) an additional TLE band is observed at around 450 nm. The TLE bands at 450 and 340 nm are attributed to the transition from the 4f ground level to the lowest 5d level ($5d_1$) and the second lowest 5d level ($5d_2$), respectively. Because trap filling proceeds by electron transport through the conduction band, these results provide evidence that electrons in the $5d_2$ level are thermally ionized to the conduction band already at 303 K (30 °C), but electrons at the $5d_1$ level are only thermally ionized efficiently at higher temperatures of around 573 K (300 °C).

The glow curves for estimating activation energies of thermal ionization process are collected in Figure 4, showing the change

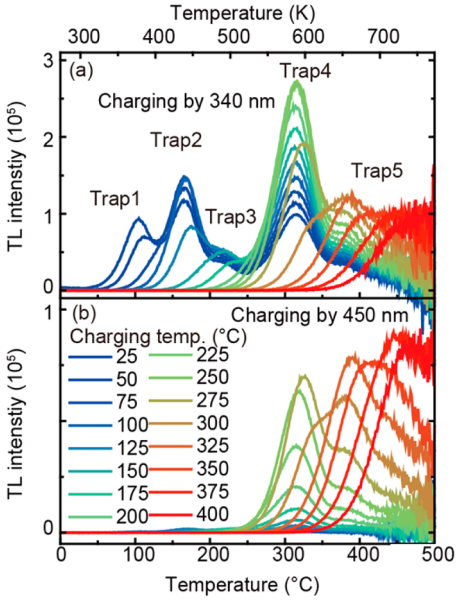

Figure 4. Corrected TL glow curves after charging by (a) 340 and (b) 450 nm at various charging temperatures varying from 298 (25 °C) to 673 K (400 °C).

of the TL glow curves with charging temperature under 340 (Figure 4a) and 450 nm (Figure 4b) illumination, which correspond to the 4f−$5d_2$ and 4f−$5d_1$ absorption, respectively. The sample was cooled down to room temperature after illumination at the charging temperature, and then the TL glow curve was recorded. In the analysis of the change of TL intensity by the thermally activated ionization at different temperatures, only the TL peak related to trap 5 was integrated because this TL peak is not affected by the thermal detrapping up to approximately 623 K (300 °C). The TL intensity related to trap 5 as a function of charging temperature after 450 nm illumination is shown in Figure 1b as filled red circles. With increasing temperature, the peak 5 TL intensity increases while the Ce^{3+} PL intensity decreases. This correlated opposite tendency strongly indicates that the mechanism responsible for the thermal quenching of the Ce^{3+} luminescence is thermal ionization.

To estimate the thermal activation energy for the thermal ionization, Figure 5 shows the Arrhenius plot of peak 5 TL

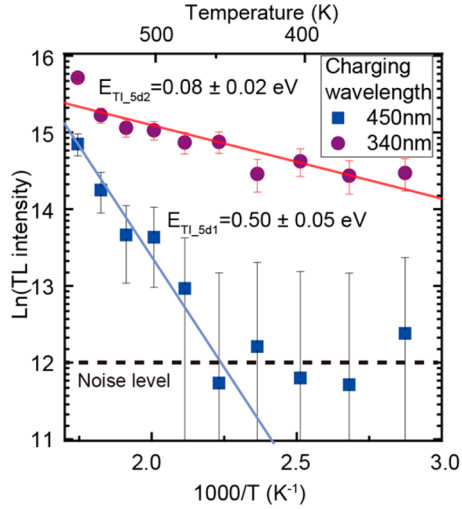

Figure 5. Arrhenius plot of TL intensity related to trap 5 charged by 340 and 450 nm.

intensity under 340 and 450 nm charging. Since trap 5 can be partially detrapped above 573 K (300 °C) and the TL peak is not observed below 423 K (for 450 nm charging), temperature ranges of 423−573 and 348−573 K are selected for the Arrhenius analysis of the results under 450 and 350 nm illumination, respectively. From the linear dependence in the Arrhenius plots in Figure 5 activation energies for thermal ionization under charging by 340 and 450 nm illumination, E_{TI_5d2} and E_{TI_5d1}, were estimated to be 0.08 ± 0.02 and 0.50 ± 0.05 eV, respectively. This result can be explained using the energy location of $5d_1$, $5d_2$, and CB as shown in the vacuum-referred binding energy (VRBE) diagram in Figure 6. The VRBE diagram is constructed using the data by our group.[27,30] To indicate the trap levels, we simply subtracted the obtained trap depth energies from the energy at the bottom of the CB. The $5d_1$-CB energy gap is much larger than the $5d_2$-CB energy gap in the VRBE diagram. Thus, the activation energy from $5d_1$ is much larger. The activation energy of 0.5 eV for 450 nm charging is slightly smaller than the activation energies of 0.79 ± 0.01 and 0.76 ± 0.02 eV estimated from lifetime and PL intensity in Figure 1, respectively. This is probably because the charging temperature affects not only the thermal ionization

DOI: 10.1021/acs.jpcc.5b08828
J. Phys. Chem. C XXXX, XXX, XXX−XXX

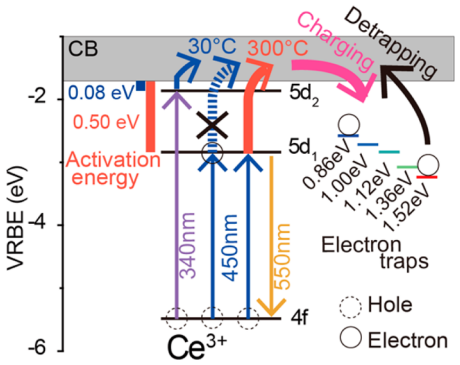

Figure 6. Vacuum-referred binding energy (VRBE) diagram of YAG:Ce^{3+} showing the energies of the 4f ground state and the $5d_1$ and $5d_2$ states of Ce^{3+} as well as the conduction band (CB) of the YAG host. Energy differences (thermal activation energies) between the 5d excited states and the bottom of the CB, as deduced from the TLE experiments in this report, are indicated as well as the thermal trap depths of traps 1−5 estimated from TL glow curves. On the basis of the large thermal activation energy from the $5d_1$ state to the CB, thermally activated photoionization is not possible at 30 °C but can explain thermal quenching starting at 300 °C.

probability from the 5d levels to the CB but also trapping probability from the CB to the traps. In addition, the band gap is known to be temperature dependent, which can also result in a variation of the $5d_1$-CB energy gap with temperature and affect the activation energy. These activation energies are also different from the $5d_1$-CB energy gap of 1.1−1.2 eV estimated from the threshold energy of photoconductivity,[19,26] ESA analysis,[16] and the VRBE diagram.[27] The differences between the activation energy estimated in the temperature dependence of PL and lifetime (related to thermally activated processes) and the $5d_1$-CB energy gap from the three analysis methods based on optical excitation can be related to the lattice relaxation. Optical excitation occurs to an unrelaxed higher vibrational state according to Franck−Condon principle, while thermal activation energies correspond to energy differences between the electronic origins of relaxed states.

On the basis of the relatively large activation energy barrier from $5d_1$ to the CB, the excited electron at the $5d_1$ band cannot be transferred to the CB at room temperature efficiently while at 573 K (300 °C) thermally activated release into the CB is possible. From these results, we can assume that when the energy difference between the lowest 5d excited level and the CB is around 1 eV in a VRBE diagram, the quenching due to thermally activated photoionization can be expected around 573 K (300 °C). This relationship between the $5d_1$-CB energy gap and the onset quenching temperature can also be applied to explain the thermal quenching behavior for other Ce^{3+}- or Eu^{2+}-doped phosphors.

4. CONCLUSIONS

To elucidate the mechanism of thermal quenching of the Ce^{3+} luminescence in the prominent LED phosphor YAG:Ce^{3+}, thermoluminescence excitation (TLE) spectra were recorded at 303 (30 °C) and 573 K (300 °C). At 30 °C only the higher energy $5d_2$ band at 340 nm gives rise to thermal ionization, as evidenced by the observation of a TL signal after 340 nm photoexcitation. At 300 °C, a temperature corresponding to the onset of thermal quenching of the Ce^{3+} luminescence, excitation in the lowest $5d_1$ band at 450 nm gives rise to a TL signal, indicating that thermal ionization is responsible for thermal quenching of the Ce^{3+} luminescence. Temperature-dependent measurements show an excellent correspondence between the thermal quenching of the Ce^{3+} luminescence and the rise of the TL signal in the temperature range 500−700 K. This confirms that thermal ionization and not thermally activated cross over to the 4f ground state is the mechanism responsible for the thermal quenching of the yellow emission in the YAG:Ce^{3+} phosphor.

A band diagram with the positions of the $5d_1$ and $5d_2$ states of Ce^{3+} relative to the YAG host conduction band confirm the analysis. Activation energies are in line with previous estimates of the energy differences between the 5d levels of Ce^{3+} and the CB of the host. The present results can aid in further improving the thermal stability of the Ce^{3+} luminescence in garnets through band-gap engineering and can also serve to provide guidelines to relate optical and thermal activation energies between localized 5d states of Ce^{3+} and Eu^{2+} and the host conduction band to luminescence quenching temperatures.

AUTHOR INFORMATION

Corresponding Author

*E-mail: ueda.jumpei.5r@kyoto-u.ac.jp.

Author Contributions

The manuscript was written through contributions of all authors.

Notes

The authors declare no competing financial interest.

ACKNOWLEDGMENTS

This work was supported by the Project of Strategic Young Researcher Overseas Visits Program for Accelerating Brain Circulation (International Network-hub for Future Earth: Research for Global Sustainability).

REFERENCES

(1) Akasaki, I.; Amano, H.; Nakamura, S. The Nobel Prize in Physics 2014. Nobel Media AB [Online] 2014; http://www.nobelprize.org/nobel_prizes/physics/laureates/2014/ (accessed Aug 1, 2015).

(2) Bando, K.; Sakano, K.; Noguchi, Y.; Shimizu, Y. Development of High-bright and Pure-white LED Lamps. *J. Light Visual Environ.* **1998**, *22*, 2−4.

(3) Setlur, A. A. Phosphors for LED-based Solid-State Lighting. *J. Electrochem. Soc. Interface* **2009**, *18*, 32−36.

(4) Lin, C. C.; Liu, R.-S. Advances in Phosphors for Light-Emitting Diodes. *J. Phys. Chem. Lett.* **2011**, *2*, 1268−1277.

(5) Blasse, G.; Bril, A. A New Phosphor for Flying-Spot Cathode-Ray Tubes for Color Television: Yellow-Emitting $Y_3Al_5O_{12}$−Ce^{3+}. *Appl. Phys. Lett.* **1967**, *11*, 53−55.

(6) Holloway, W. W., Jr.; Kestigian, M. Optical Properties of Cerium-Activated Garnet Crystals. *J. Opt. Soc. Am.* **1969**, *59*, 60−63.

(7) Nishiura, S.; Tanabe, S.; Fujioka, K.; Fujimoto, Y. Properties of Transparent Ce:YAG Ceramic Phosphors for White LED. *Opt. Mater.* **2011**, *33*, 688−691.

(8) Barry, T. L. Fluorescence of Eu^{2+}-Activated Phases in Binary Alkaline Earth Orthosilicate Systems. *J. Electrochem. Soc.* **1968**, *115*, 1181−1184.

(9) Kim, J. S.; Park, Y. H.; Kim, S. M.; Choi, J. C.; Park, H. L. Temperature-Dependent Emission Spectra of M_2SiO_4:Eu^{2+} (M = Ca, Sr, Ba) Phosphors for Green and Greenish White LEDs. *Solid State Commun.* **2005**, *133*, 445−448.

(10) Xie, R.-J.; Mitomo, M.; Uheda, K.; Xu, F.-F.; Akimune, Y. Preparation and Luminescence Spectra of Calcium- and Rare-Earth (R = Eu, Tb, and Pr)-Codoped α-SiAlON Ceramics. *J. Am. Ceram. Soc.* **2002**, *85*, 1229−1234.

DOI: 10.1021/acs.jpcc.5b08828
J. Phys. Chem. C XXXX, XXX, XXX−XXX

(11) Park, S.; Vogt, T. Defect Monitoring and Substitutions in $Sr_{3-x}A_xAlO_4F$ (A = Ca, Ba) Oxyfluoride Host Lattices and Phosphors. *J. Phys. Chem. C* **2010**, *114*, 11576−11583.
(12) Kim, T.-G.; Kim, T.; Kim, J.; Kim, S.-J.; Im, S.-J. Interplay between Crystal Structure and Photoluminescence Properties of β-$Ca_3SiO_4Cl_2$:Eu^{2+}. *J. Phys. Chem. C* **2014**, *118*, 12428−12435.
(13) Lv, W.; Jia, Y.; Zhao, Q.; Lü, W.; Jiao, M.; Shao, B.; You, H. Synthesis, Structure, and Luminescence Properties of $K_2Ba_7Si_{16}O_{40}$:Eu^{2+} for White Light Emitting Diodes. *J. Phys. Chem. C* **2014**, *118*, 4649−4655.
(14) Xia, Z.; Zhang, Y.; Molokeev, M. S.; Atuchin, V. V. Structural and Luminescence Properties of Yellow-Emitting $NaScSi_2O_6$:Eu^{2+} Phosphors: Eu^{2+} Site Preference Analysis and Generation of Red Emission by Codoping Mn^{2+} for White-Light-Emitting Diode Applications. *J. Phys. Chem. C* **2013**, *117*, 20847−20854.
(15) Ueda, J.; Aishima, K.; Tanabe, S. Temperature and Compositional Dependence of Optical and Optoelectronic Properties in Ce^{3+}-Doped $Y_3Sc_2Al_{3-x}Ga_xO_{12}$ (x = 0, 1, 2, 3). *Opt. Mater.* **2013**, *35*, 1952−1957.
(16) Struck, C.; Fonger, W. *Understanding Luminescence Spectra and Efficiency Using W p and Related Functions*; Springer: Berlin, Germany, 1991; Vol. *13*.
(17) Yen, W. M.; Raukas, M.; Basun, S. A.; van Schaik, W.; Happek, U. Optical and Photoconductive Properties of Cerium-Doped Crystalline Solids. *J. Lumin.* **1996**, *69*, 287−294.
(18) Chiang, C. C.; Tsai, M. S.; Hon, M. H. Luminescent Properties of Cerium-Activated Garnet Series Phosphor: Structure and Temperature Effects. *J. Electrochem. Soc.* **2008**, *155*, B517−B520.
(19) Ueda, J.; Tanabe, S.; Nakanishi, T. Analysis of Ce^{3+} Luminescence Quenching in Solid Solutions between $Y_3Al_5O_{12}$ and $Y_3Ga_5O_{12}$ by Temperature Dependence of Photoconductivity Measurement. *J. Appl. Phys.* **2011**, *110*, 053102.
(20) Ogiegło, J. M.; Katelnikovas, A.; Zych, A.; Jüstel, T.; Meijerink, A.; Ronda, C. R. Luminescence and Luminescence Quenching in $Gd_3(Ga,Al)_5O_{12}$ Scintillators Doped with Ce^{3+}. *J. Phys. Chem. A* **2013**, *117*, 2479−2484.
(21) Zhong, J.; Zhuang, W.; Xing, X.; Liu, R.; Li, Y.; Liu, Y.; Hu, Y. Synthesis, Crystal Structures, and Photoluminescence Properties of Ce^{3+}-Doped $Ca_2LaZr_2Ga_3O_{12}$: New Garnet Green-Emitting Phosphors for White LEDs. *J. Phys. Chem. C* **2015**, *119*, 5562−5569.
(22) Weber, M. J. Nonradiative Decay from 5d States of Rare Earths in Crystals. *Solid State Commun.* **1973**, *12*, 741−744.
(23) Lyu, L.-J.; Hamilton, D. S. Radiative and Nonradiative Relaxation Measurements in Ce^{3+} Doped Crystals. *J. Lumin.* **1991**, *48−49*, 251−254.
(24) Bachmann, V.; Ronda, C.; Meijerink, A. Temperature Quenching of Yellow Ce^{3+} Luminescence in YAG:Ce. *Chem. Mater.* **2009**, *21*, 2077−2084.
(25) Hamilton, D. S.; Gayen, S. K.; Pogatshnik, G. J.; Ghen, R. D.; Miniscalco, W. J. Optical-Absorption and Photoionization Measurements from the Excited States of Ce^{3+}:$Y_3Al_5O_{12}$. *Phys. Rev. B: Condens. Matter Mater. Phys.* **1989**, *39*, 8807−8815.
(26) Pedrini, C.; Rogemond, F.; McClure, D. S. Photoionization Thresholds of Rare-earth Impurity Ions. Eu^{2+}:CaF_2, Ce^{3+}:YAG, and Sm^{2+}:CaF_2. *J. Appl. Phys.* **1986**, *59*, 1196−1201.
(27) Dorenbos, P. Electronic Structure and Optical Properties of the Lanthanide Activated $RE_3(Al_{1-x}Ga_x)_5O_{12}$ (RE = Gd, Y, Lu) Garnet Compounds. *J. Lumin.* **2013**, *134*, 310−318.
(28) Ivanovskikh, K. V.; Ogiegło, J. M.; Zych, A.; Ronda, C. R.; Meijerink, A. Luminescence Temperature Quenching for Ce^{3+} and Pr^{3+} d-f Emission in YAG and LuAG. *ECS J. Solid State Sci. Technol.* **2013**, *2*, R3148−R3152.
(29) Bos, A. J. J.; van Duijvenvoorde, R. M.; van der Kolk, E.; Drozdowski, W.; Dorenbos, P. Thermoluminescence Excitation Spectroscopy: A Versatile Technique to Study Persistent Luminescence Phosphors. *J. Lumin.* **2011**, *131*, 1465−1471.
(30) Ueda, J.; Dorenbos, P.; Bos, A. J. J.; Kuroishi, K.; Tanabe, S. Control of Electron Transfer between Ce^{3+} and Cr^{3+} in the $Y_3Al_{5-x}Ga_xO_{12}$ Host via Conduction Band Engineering. *J. Mater. Chem. C* **2015**, *3*, 5642−5651.
(31) Randall, J. T.; Wilkins, M. H. F. Phosphorescence and Electron Traps. I. The Study of Trap Distributions. *Proc. R. Soc. London, Ser. A* **1945**, *184*, 365−389.
(32) Randall, J. T.; Wilkins, M. H. F. Phosphorescence and Electron Traps. II. The Interpretation of Long-Period Phosphorescence. *Proc. R. Soc. London, Ser. A* **1945**, *184*, 390−407.
(33) Bos, A. J. J. Theory of Thermoluminescence. *Radiat. Meas.* **2006**, *41*, S45−S56.
(34) Rodríguez-Rojas, R. A.; De la Rosa-Cruz, E.; Díaz-Torres, L. A.; Salas, P.; Meléndrez, R.; Barboza-Flores, M.; Meneses-Nava, M. A.; Barbosa-García, O. Preparation, Photo- and Thermo-Luminescence Characterization of Tb^{3+} and Ce^{3+} Doped Nanocrystalline $Y_3Al_5O_{12}$ Exposed to UV-irradiation. *Opt. Mater.* **2004**, *25*, 285−293.
(35) Rodríguez, R. A.; De la Rosa, E.; Díaz-Torres, L. A.; Salas, P.; Meléndrez, R.; Barboza-Flores, M. Thermoluminescence Characterization of Tb^{3+} and Ce^{3+} Doped Nanocrystalline $Y_3Al_5O_{12}$ Exposed to X- and β-ray Irradiation. *Opt. Mater.* **2004**, *27*, 293−299.
(36) Wisniewski, K.; Koepke, C.; Wojtowicz, A. J.; Drozdowski, W.; Grinberg, M.; Kaczmarek, S. M.; Kisielewski, J. Excited State Absorption and Thermoluminescence in Ce and Mg Doped Yttrium Aluminium Garnet. *Acta Phys. Polym., A* **1999**, *95*, 403−412.
(37) Zhang, S.; Li, C.; Pang, R.; Jiang, L.; Shi, L.; Su, Q. Long-Lasting Phosphorescence Study on $Y_3Al_5O_{12}$ Doped with Different Concentrations of Ce^{3+}. *J. Rare Earths* **2011**, *29*, 426−430.

DOI: 10.1021/acs.jpcc.5b08828
J. Phys. Chem. C XXXX, XXX, XXX−XXX